

# The initial gluon multiplicity in heavy ion collisions.

Alex Krasnitz

*UCEH, Universidade do Algarve, Campus de Gambelas, P-8000 Faro, Portugal.*

Raju Venugopalan

*Physics Department, Brookhaven National Laboratory, Upton, NY 11973, USA.*

October 31, 2018

## Abstract

The initial gluon multiplicity per unit area per unit rapidity,  $dN/L^2/d\eta$ , in high energy nuclear collisions, is equal to  $f_N(g^2\mu L)(g^2\mu)^2/g^2$ , with  $\mu^2$  proportional to the gluon density per unit area of the colliding nuclei. For an SU(2) gauge theory, we compute  $f_N(g^2\mu L) = 0.14 \pm 0.01$  for a wide range in  $g^2\mu L$ . Extrapolating to SU(3), we predict  $dN/L^2/d\eta$  for values of  $g^2\mu L$  in the range relevant to the Relativistic Heavy Ion Collider and the Large Hadron Collider. We compute the initial gluon transverse momentum distribution,  $dN/L^2/d^2k_\perp$ , and show it to be well behaved at low  $k_\perp$ .

A topic of considerable current interest is the possibility of forming an equilibrated plasma of quarks and gluons, a quark–gluon plasma (QGP), in very high energy nuclear collisions. Experimental signatures of such a plasma may provide insight into the nature of the QCD phase diagram at finite temperature and baryon density [1].

Equally interesting, is the information that heavy ion collisions may provide about the distributions of partons in the wavefunctions of the nuclei *before* the collision. At very high energies, the growth of parton distributions in the nuclear wavefunction saturates, forming a state of matter sometimes called a Color Glass Condensate (CGC) [2]. The condensate is characterized by a bulk momentum scale  $Q_s$ . If  $Q_s \gg \Lambda_{QCD}$ , the properties of this condensate, albeit non-perturbative, can be studied in weak coupling. The partons that comprise this condensate are freed in a collision. Since the scale of the condensate,  $Q_s$ , is the only scale in the problem, the initial multiplicity and energy distributions of produced gluons at central rapidities are determined by this scale alone. We will briefly discuss later the relation of these quantities to physical observables.

The above statements may be quantified in a classical effective field theory approach (EFT) to high energy scattering [4]. The EFT is classical because, at central rapidities, where  $x \ll 1$  and  $p_\perp \gg \Lambda_{QCD}$ , ( $x \sim p_\perp/\sqrt{s}$ ), parton distributions grow rapidly with

decreasing  $x$  giving rise to large occupation numbers. Briefly, the EFT separates partons in a hadron (or nucleus) into static, high  $x$  valence and hard glue sources, and “wee” small  $x$  fields. For a large nucleus in the infinite momentum frame, the hard sources with color charge density  $\rho$ , are randomly distributed in the transverse plane with the distribution

$$P([\rho]) = \exp\left(-\frac{1}{2g^4\mu^2} \int d^2x_\perp \rho^2(x_\perp)\right). \quad (1)$$

The average squared color charge per unit area is determined by the parameter  $\mu^2$ , which is the only dimensional parameter in the EFT apart from the linear size  $L$  of the nucleus. Parton distributions, correlation functions of the wee gauge fields, are computed by averaging over gauge fields with the weight  $P([\rho])$  [5].

Quantum corrections to the EFT [6] are implemented using Wilson renormalization group techniques [7]. The scale  $\mu^2$  grows with decreasing  $x$ , and can be estimated from the *nucleon* quark and gluon distributions at  $x \ll 1$  [9]. The saturation scale — at which parton distributions stop growing rapidly with decreasing  $x$  — is  $Q_s \sim 6g^2\mu/4\pi$  [3], a function determined self-consistently from the typical  $x$  and  $Q^2$  of interest. Since most of the saturated partons have momenta of this order,  $Q_s$ , rather than  $g^2\mu$ , is the appropriate scale. At RHIC energies,  $Q_s \sim 1$  GeV, and at LHC,  $Q_s \sim 2$ –3 GeV. The magnitude of  $Q_s$  is a rough estimate because of our uncertain knowledge of gluon structure functions at these energies. This scale, and the properties of the CGC, may be further determined in future high energy deeply inelastic scattering (DIS) experiments off nuclei [8].

In this letter, we obtain a non-perturbative relation between the multiplicity of gluons produced in heavy ion collisions at central rapidities on the one hand, and  $g^2\mu$ , or equivalently  $Q_s$ , on the other. We will also demonstrate that non-perturbative strong field effects, at momenta  $k_\perp \sim Q_s$ , qualitatively alter transverse momentum distributions, rendering them infrared finite. A preliminary version of these results was reported in Ref. [14]. In a previous letter [15], we obtained a similar expression for the energy of gluons, per unit rapidity, produced shortly after a very high energy nuclear collision.

The problem of initial conditions [16] for nuclear scattering can be formulated in the classical EFT [10] in the gauge  $A^\tau = 0$ . Matching the Yang–Mills equations  $D_\mu F^{\mu\nu} = J^\nu$  in the four light cone regions, along the light cone, one obtains for the gauge fields in the forward light cone, at proper time  $\tau = 0$ , the relations  $A^i = A_1^i + A_2^i$  and  $A^\pm = \pm igx^\pm [A_1^i, A_2^i]/2$ . Here  $J^\nu = \Sigma_{1,2} \delta^{\nu,\pm} \delta(x^\mp) \rho^{1,2}(x_\perp)$  are random light cone sources corresponding to the valence or hard glue sources in the two nuclei. The transverse pure gauge fields  $A_{1,2}^i(\rho^\pm)$ , with  $i = 1, 2$  are solutions of the Yang–Mills equations for each of the two nuclei before the collision. With these initial conditions, the Yang–Mills equations can be solved in the forward light cone to obtain gluon configurations at late proper times. Since the initial conditions depend on the sources  $\rho^\pm$ , averages over different realizations of the sources — specified by the weight in Eq. (1) — must be performed.

Perturbative solutions for the number distributions in transverse momentum, per unit rapidity, were obtained in Refs. [10, 11]. These were shown to be infrared divergent.

In the classical EFT, this divergence is logarithmic. The number distributions have the form

$$n_{k_{\perp}} \propto \frac{1}{\alpha_S} \left( \frac{\alpha_S \mu}{k_{\perp}} \right)^4 \ln \left( \frac{k_{\perp}}{\alpha_S \mu} \right), \quad (2)$$

for  $k_{\perp} \gg \alpha_S \mu$ . The perturbative description breaks down at  $k_{\perp} \sim \alpha_S \mu$ . Thus, for robust predictions of gluon multiplicity distributions, a fully non-perturbative study of the classical EFT is necessary [12].

The model is discretized on a lattice in the transverse momentum plane. Boost invariance and periodic boundary conditions are assumed. The lattice Hamiltonian is the Kogut–Susskind Hamiltonian in 2+1–dimensions coupled to an adjoint scalar field. The lattice field equations are then solved by computing the Poisson brackets, with initial conditions that are the lattice analogs of the continuum initial conditions mentioned earlier. Technical details of our simulations can be found in Refs. [13, 15]. Our simulations are presently only for an SU(2) gauge theory — the full SU(3) case will be studied later.

The scale  $g^2 \mu$  and the linear size of the nucleus  $L$  are the only physically relevant dimensional parameters of the classical EFT. Any dimensional quantity  $P$  well defined within the EFT can then be written as  $(g^2 \mu)^d f_P(g^2 \mu L)$ , where  $d$  is the dimension of  $P$ . All the non-trivial physical information is therefore contained in the dimensionless function  $f_P(g^2 \mu L)$ . On the lattice,  $P$  will generally depend on the lattice spacing  $a$ ; this dependence can be removed by taking the continuum limit  $a \rightarrow 0$ . Assuming  $g = 2$ , the physically relevant values of  $g^2 \mu$  for RHIC and LHC energies are  $\sim 2$  GeV and  $\sim 4$  GeV respectively. Also, assuming central Au–Au collisions, we obtain  $L = 11.6$  fm as the physical linear dimension of our square lattice. Thus,  $g^2 \mu L \approx 120$  (240) for RHIC (LHC). In Ref. [15], we computed the initial energy density, per unit area per unit rapidity, to be  $dE/L^2/d\eta = f_E(g^2 \mu)^3$ . We computed  $f_E$  as a function of  $g^2 \mu L$ , and extrapolated our results for  $f_E$  to the continuum limit. We could however just as well express our result as  $dE/\pi R^2/d\eta = c_E(Q_s R)(Q_s)^3$ , with  $c_E \sim 4.3$ – $4.9$  in the region of interest.

We will now report on our results for the initial multiplicity of gluons produced at central rapidities in very high energy nuclear collisions. This quantity, while not directly observable, is related to the number of hadrons produced at central rapidities [20]. The initial multiplicity and momentum distribution of gluons also determine the equilibration time, the temperature and the chemical potential of the QGP [17, 24]. The various signatures of QGP formation are highly sensitive to these quantities [1].

We must first clarify what we mean by the number of quanta in the interacting, non-Abelian gauge theory at hand. To motivate the discussion, let us first consider a free field theory whose Hamiltonian in momentum space has the form

$$H_f = \frac{1}{2} \sum_k \left( |\pi(k)|^2 + \omega^2(k) |\phi(k)|^2 \right), \quad (3)$$

where  $\phi(k)$  is the  $k$ th momentum component of the field,  $\pi(k)$  is its conjugate momentum, and  $\omega(k)$  is the corresponding eigenfrequency. The average particle number of the  $k$ -th

mode is then

$$N(k) = \omega(k) \langle |\phi(k)|^2 \rangle = \sqrt{\langle |\phi(k)|^2 |\pi(k)|^2 \rangle}, \quad (4)$$

In our case, the average  $\langle \rangle$  is over the initial conditions.

Clearly, any extension of this notion to interacting theories should reduce to the standard free-field definition of the particle number in the weak coupling limit. However, this requirement alone does not define the particle number uniquely outside a free theory. We therefore use two different generalizations of the particle number to an interacting theory. Each has the correct free-field limit. Even though the fields in question are strongly interacting at early times, they are only weakly coupled at late times, and it is only at this stage that it becomes reasonable to define particle number. We verify that the two definitions agree in this weak-coupling regime.

Our first definition of the multiplicity is straightforward. We impose the Coulomb gauge condition in the transverse plane,  $\vec{\nabla}_\perp \cdot \vec{A}_\perp = 0$ , and substitute the momentum components of the resulting field configuration into Eq. (4). One option now is to assume  $\omega(k_\perp)$  to be the standard massless (lattice) dispersion relation and use the middle expression of Eq. (4) to compute  $N(k_\perp)$ . Alternatively, we can determine  $N(k_\perp)$  from the rightmost expression of Eq. (4); the middle expression of Eq. (4) can then be used to obtain  $\omega(k_\perp)$ . The second option is preferable; it does not require us to assume that the dispersion relation is linear.

Our second definition is based on the behavior of a free-field theory under cooling. Consider a simple relaxation equation for a field in real space,

$$\partial_t \phi(x) = -\partial H / \partial \phi(x), \quad (5)$$

where  $t$  is the cooling time (*not to be confused with real or proper time*) and  $H$  is the Hamiltonian. For a free field theory ( $H = H_f$ ) the relaxation equation has exactly the same form in the momentum space with the solution  $\phi(k, t) = \phi(k, 0) \exp(-\omega^2(k)t)$ . The potential energy of the relaxed free field is  $V(t) = (1/2) \sum_k \omega^2(k) |\phi(k, t)|^2$ . It is then easy to derive the following integral expression for the total particle number of a free-field system:

$$N = \sqrt{\frac{8}{\pi}} \int_0^\infty \frac{dt}{\sqrt{t}} V(t). \quad (6)$$

Eq. (5) can be solved numerically for interacting fields. Subsequently,  $V(t)$  can be determined, and  $N$  can be computed by numerical integration. Note that in a gauge theory the relaxation equations are gauge-covariant, and the relaxed potential  $V(t)$  is gauge-invariant, entailing gauge invariance of this definition of the particle number. This is an attractive feature of the cooling method. On the other hand, unlike the Coulomb gauge computation discussed earlier, this cooling technique presently only permits determination of the total particle number. It cannot be used to find the number distribution  $N(k_\perp)$ .

Both our definitions cease to make sense if the system is far from linearity. In particular, if the theory has metastable states, and the system relaxes to one of these states,

the right hand side of (6) will diverge. The expression in Eq. (4) can then still be formally determined in the Coulomb gauge but its interpretation as a particle number is problematic. This situation deserves special attention and will be discussed in detail elsewhere. We did not observe any effects of metastability within the range of parameters of the current numerical study. In particular, we verified the convergence of Eq. (6) with respect to the upper limit of integration.

We now present our results using both the techniques discussed. We begin with the number distribution, which can only be computed in Coulomb gauge. We have verified, for  $g^2\mu L = 35.35$ , that in the range of values of  $g^2\mu a$  considered here the system is close to the continuum limit. This is consistent with our earlier analysis of the lattice spacing dependence of a more ultraviolet-sensitive quantity, the energy density [15]. In Fig. 1a, we plot the gluon number distribution,  $n(k_\perp) \equiv dN/L^2/dk_\perp^2 = N(k_\perp)/(2\pi)^2$  versus  $k_\perp$  for fixed  $g^2\mu L = 35.5$ , but for different values of the lattice spacing  $g^2\mu a$ . For large  $k_\perp$ , the finest lattice ( $g^2\mu a = 0.138$ ) agrees well with the lattice perturbation theory (LPTh) analogue of Eq. (2). At smaller  $k_\perp$ , the distribution is softer, and converges to a constant value. In Fig. 1b, we plot the gluon distribution in the infrared, at fixed  $g^2\mu a$ , for different  $g^2\mu L$  (148.5 and 297). We notice that these distributions are nearly universal and independent of  $g^2\mu L$ ! Also, the convergence of the distribution to a constant value is more clearly visible in Fig. 1b.

When  $k_\perp \leq g^2\mu$ , non-perturbative effects qualitatively alter the perturbative number distribution, rendering it finite in the infrared. Unfortunately, since these effects are large, an analytical understanding of the behavior at low  $k_\perp$  is lacking. Our results, despite being universal, are not simply fit by any of the physically motivated parametrizations we have considered.

From our previous discussion, the formula

$$\frac{1}{L^2} \frac{dN}{d\eta} = \frac{1}{g^2} f_N(g^2\mu L) (g^2\mu)^2, \quad (7)$$

relates the number of produced gluons per unit area per unit rapidity at zero rapidity to  $g^2\mu$ . We have computed  $f_N$  on the lattice using the two techniques discussed earlier. Our result for  $f_N$  as a function of  $g^2\mu L$ , for the smallest values of  $g^2\mu a$  feasible, are plotted in Fig. 2. We see that the agreement between the cooling and Coulomb techniques at larger values of  $g^2\mu L$  is excellent. It is not as good at the smaller values – in general, the cooling number is more reliable [18]. We also note that Fig. 2 demonstrates that the distributions in Fig. 1b are not quite universal — otherwise,  $f_N$  would be a constant. We see instead that it has a weak logarithmic rise with  $g^2\mu L$  for larger  $g^2\mu L$ 's. Table 1 lists  $f_N$  for various  $g^2\mu L$ . The third row is the Coulomb gauge number after cooling — see Ref. [18].

In Fig. 3, we plot the dispersion relation  $\omega(k_\perp)$  vs  $k_\perp$  using the relation Eq. (4). All the dispersion curves rapidly approach the  $\omega(k_\perp) = k_\perp$  asymptote characteristic of on-shell partons, while exhibiting a mass gap at zero momentum. We reserve for a later work a detailed study of this mass gap and its role in rendering the number distributions infrared finite.

$g^2\mu L$	35.36	70.71	106.1	148.5	212.1	297.0
$g^2\mu a$	.276	.276	0.207	.29	.41	.29
$f_N$ (cooling)	$.116 \pm .001$	$.119 \pm .001$	$.127 \pm .001$	$.138 \pm .001$	$.146 \pm .001$	$.151 \pm .001$
$f_N$ (Coulomb)	$.127 \pm .002$	$.125 \pm .002$	$.135 \pm 0.001$	$142 \pm .001$	$.145 \pm .001$	$.153 \pm .001$
$f_N$ (res.) $\times 10^3$	$14 \pm 2$	$7.8 \pm 0.2$	$8.9 \pm 0.2$	$5.6 \pm 0.1$	$7.12 \pm 0.08$	$4.83 \pm .04$

Table 1: Values of  $f_N$  vs  $g^2\mu L$ , for fixed  $g^2\mu a$ , plotted in Fig. 2.  $f_N$  (res.) is defined in Ref. [18].

We can compare our results for the number distribution to the one predicted by A. H. Mueller [17]. In terms of  $Q_s$  and  $R$ , we can re-write Eq. 7 as

$$\frac{1}{\pi R^2} \frac{dN}{d\eta} = c_N \frac{N_c^2 - 1}{N_c} \frac{1}{4\pi^2\alpha_S} Q_s^2.$$

Mueller estimates the non-perturbative coefficient  $c_N$  to be of order unity. If we take  $f_N = 0.14 \pm 0.01$ , as is the case for much of the range studied, we find  $c_N = 1.29 \pm 0.09$ , a number of order unity as predicted by Mueller. Despite this close agreement, the transverse momentum distributions, shown in Fig. 1a and 1b, and discussed earlier, look quite different from Mueller's guess of  $\theta(Q_s^2 - k_\perp^2)$ . The  $\theta$ -function distribution was only a rough guess to represent a qualitative change of the distributions at  $k_\perp \sim Q_s$ .

A large number of models of particle production in nuclear collisions at RHIC and LHC energies can be found in the literature. A nice recent summary of their various predictions and relevant references can be found in the compilation of Ref. [21]. Naively extrapolating our results to SU(3), we find for  $Au$ - $Au$  central collisions at RHIC energies,  $dN/d\eta \sim 950$  for  $f_N = 0.132 \pm 0.006$  ( $g^2\mu L \approx 120$  — we take the mean of the 106 and 148 cooling point). Similarly, for LHC energies  $f_N = 0.148 \pm 0.002$  ( $g^2\mu L \sim 255$  — the mean of the 212 and 297 cooling point), one finds  $dN/d\eta \sim 4300$ . In particular, comparing our predictions with those of pQCD based models [19], we find our numbers to be in rough agreement. However, if we include a  $K$  factor like many of these models do, our numbers will be roughly a factor of 2 larger.

There is considerable uncertainty in the value of  $Q_s$  because the gluon densities at the relevant  $x$  and  $Q^2$  are ill-known. Since the multiplicity depends quadratically on  $Q_s$ , a prediction of the same is perforce unreliable. Distinguishing between different models will therefore require, at the very least, testing their predictions for the scaling of multiplicities with  $A$  and with  $\sqrt{s}$ . In our case,  $Q_s \sim A^{1/6}$ , hence from Eq. 7 the number per unit rapidity will, up to logarithms of  $A$ , be proportional to  $A$ . In the EFT, one naively expects the energy dependence to be a power law, the power being determined by the rise in the gluon density at small  $x$ . Quantitative estimates of the dependence of  $Q_s$  with energy in the saturation region are being developed. Predictions from other models vary significantly, ranging from a power law dependence [22] of  $Q_s$  to  $Q_s \propto \exp(\sqrt{\ln(s/s_0)})$ , where  $s_0$  is a constant. In the latter case [23], it is claimed that a good fit to the multiplicity from existing high energy hadron scattering data is obtained. Data from RHIC will help constrain the energy dependence of  $Q_s$ .

The reader should also note that our relations are derived only for the initial parton multiplicity distributions at central rapidities. These provide the initial conditions for the subsequent evolution of the system, which can be investigated in a transport approach [17, 24]. The rate of chemical equilibration, and uncertainties due to hadronization also have to be taken into account in predictions of observables such as charged hadron multiplicities. Conversely, these observables may help constrain the saturation scale  $Q_s$ , and inform us about the very earliest stages of nuclear collisions.

In summary, we have derived a non-perturbative relation between the multiplicity of produced partons and the saturation scale of parton distributions in high energy nuclear collisions. We have computed number distributions which have the predicted perturbative behavior in the ultraviolet, and are finite in the infrared. At present, in our approach, we are only able to make qualitative “ball-park” predictions. However, we have developed a framework in which these can be quantified and extended in a consistent manner to study a large number of final state observables in heavy ion collisions.

## Acknowledgments

We would like to thank Larry McLerran and Al Mueller for very useful discussions. R. V.’s research was supported by DOE Contract No. DE-AC02-98CH10886. The authors acknowledge support from the Portuguese FCT, under grants CERN/P/FIS/1203/98 and CERN/P/FIS/15196/1999.

## References

- [1] see for instance, the proceedings of *Quark Matter 99*, *Nucl. Phys.* **A661** (1999).
- [2] Larry McLerran, private communication.
- [3] A. H. Mueller, *Nucl. Phys.* **558** 285 (1999); R. Venugopalan, hep-ph/9907209.
- [4] L. McLerran and R. Venugopalan, *Phys. Rev.* **D49** 2233 (1994); **D49** 3352 (1994); **D50** 2225 (1994).
- [5] Hence the analogy to spin glasses. See R. V. Gavai and R. Venugopalan, *Phys. Rev.* **D54** 5795 (1996).
- [6] A. Ayala, J. Jalilian-Marian, L. McLerran, and R. Venugopalan, *Phys. Rev.* **D52**, 2935 (1995); *ibid.* **D53** 458 (1996).
- [7] J. Jalilian-Marian, A. Kovner, L. McLerran, and H. Weigert, *Phys. Rev.* **D55** (1997) 5414; J. Jalilian-Marian, A. Kovner, A. Leonidov, and H. Weigert, *Nucl. Phys.* **B504** 415 (1997); J. Jalilian-Marian, A. Kovner, and H. Weigert, *Phys. Rev.* **D59** 014015 (1999); L. McLerran and R. Venugopalan, *Phys. Rev.* **D59** 094002 (1999).

- [8] M. Arneodo et al., hep-ph/9610423, in *Proceedings of workshop on future physics at HERA*, Hamburg, Sept. 25th-26th, (1995); *Proceedings of the 2nd eRHIC workshop*, Yale, April 6th-8th, (2000), to be published.
- [9] M. Gyulassy and L. McLerran, *Phys. Rev.* **C56** (1997) 2219.
- [10] A. Kovner, L. McLerran and H. Weigert, *Phys. Rev* **D52** 3809 (1995); **D52** 6231 (1995).
- [11] Y. V. Kovchegov and D. H. Rischke, *Phys. Rev.* **C56** (1997) 1084; S. G. Matinyan, B. Müller and D. H. Rischke, *Phys. Rev.* **C56** (1997) 2191; *Phys. Rev.* **C57** (1998) 1927; Xiao-feng Guo, *Phys. Rev.* **D59** 094017 (1999).
- [12] A. Krasnitz and R. Venugopalan, hep-ph/9706329, hep-ph/9808332.
- [13] A. Krasnitz and R. Venugopalan, *Nucl. Phys.* **B557** 237 (1999).
- [14] A. Krasnitz and R. Venugopalan, hep-ph/0004116.
- [15] A. Krasnitz and R. Venugopalan, *Phys. Rev. Lett.* **84**, 4309 (2000).
- [16] see for instance, I. Balitsky, *Phys. Rev.* **D60** 014020 (1999); Y. V. Kovchegov and A. H. Mueller, *Nucl. Phys.* **B529** 451 (1998); S. A. Bass, B. Müller, and W. Poschl, *J. Phys. G25* L109 (1999).
- [17] A. H. Mueller, *Nucl. Phys.* **B572**, 227 (2000); *Phys. Lett.* **B475**, 220 (2000).
- [18] The discrepancy between Coulomb gauge numbers and cooling numbers is likely due to gauge artifacts. The Coulomb gauge number *after* cooling (third row of Table. 1) — in principle close to zero — added to the gauge invariant cooling number, agrees closely with the Coulomb gauge number *before* cooling.
- [19] K. J. Eskola, K. Kajantie, P. V. Ruuskanen, and K. Tuominen, *Nucl. Phys.* **B570**, 379 (2000); K. J. Eskola, B. Müller, and X-N. Wang, nucl-th/9608013; K. Geiger, *Phys. Rep.* **258** (1995) 237; X-N. Wang, *Phys. Rept.* **280**, 287 (1997); N. Hammon, H. Stocker and W. Greiner, *Phys. Rev.* **C61**, 014901 (2000).
- [20] L. McLerran, hep-ph/9903536.
- [21] N. Armesto and C. Pajares, hep-ph/0002163.
- [22] Y. V. Kovchegov, *Phys. Rev.* **D61** :074018 (2000).
- [23] E. M. Levin and M. G. Ryskin, *Phys. Repts.* **189** (1990) 267.
- [24] J. Bjorker and R. Venugopalan, in preparation.



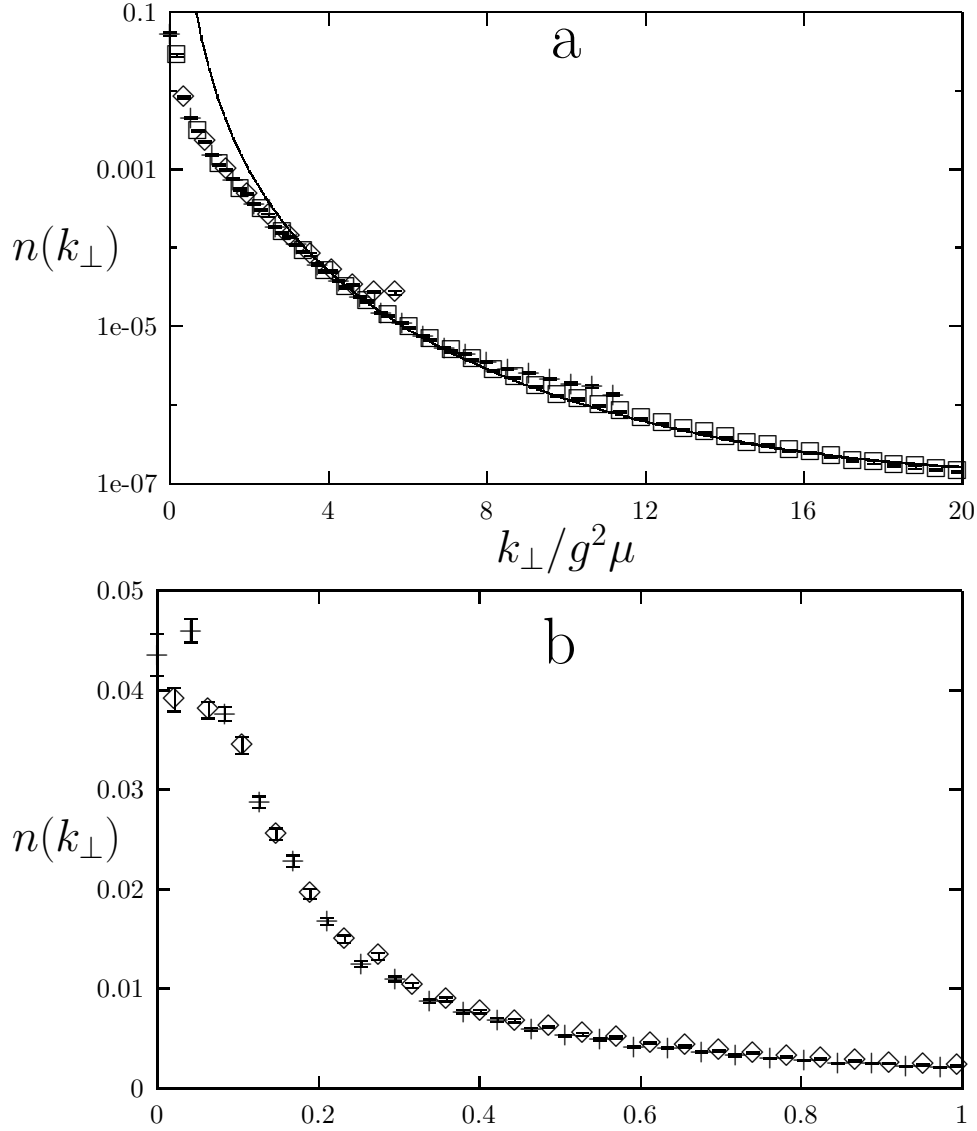


Figure 1: a:  $n(k_{\perp}) \equiv dN/L^2/d^2k_{\perp}$  as a function of the gluon momentum  $k$  for  $g^2\mu L = 35.35$  and the values 0.138 (squares), 0.276 (plusses), and 0.552 (diamonds) of  $g^2\mu a$ . The gluon momentum  $k$  is in units of  $g^2\mu$ . The solid line is a fit of the lattice analog of the perturbative expression Eq. (2) to the high-momentum part of the  $g^2\mu a = 0.138$  data. b:  $n(k_{\perp})$  at soft momenta at  $g^2\mu a = 0.29$  for the values 148.5 (plusses) and 297 (diamonds) of  $g^2\mu L$ .

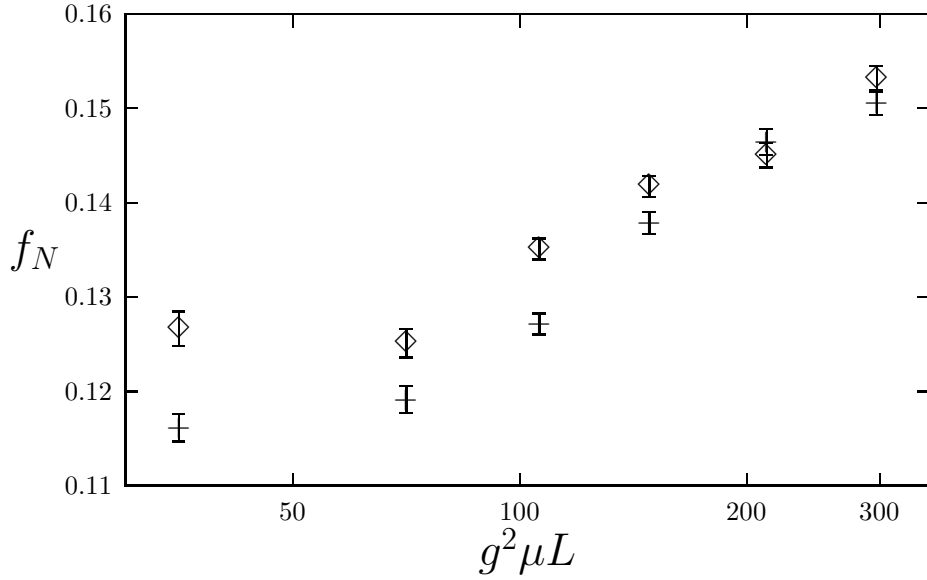


Figure 2: The function  $f_N$ , defined in Eq. (7) as a function of  $g^2 \mu L$ , obtained by the relaxation method (plusses) and by the Coulomb gauge fixing (diamonds). The values of  $g^2 \mu a$  are 0.276 for  $g^2 \mu L = 35.35$  and  $g^2 \mu L = 70.8$ ; 0.29 for  $g^2 \mu L = 148.5$  and  $g^2 \mu L = 297$ ; and 0.414 for  $g^2 \mu L = 212$ .

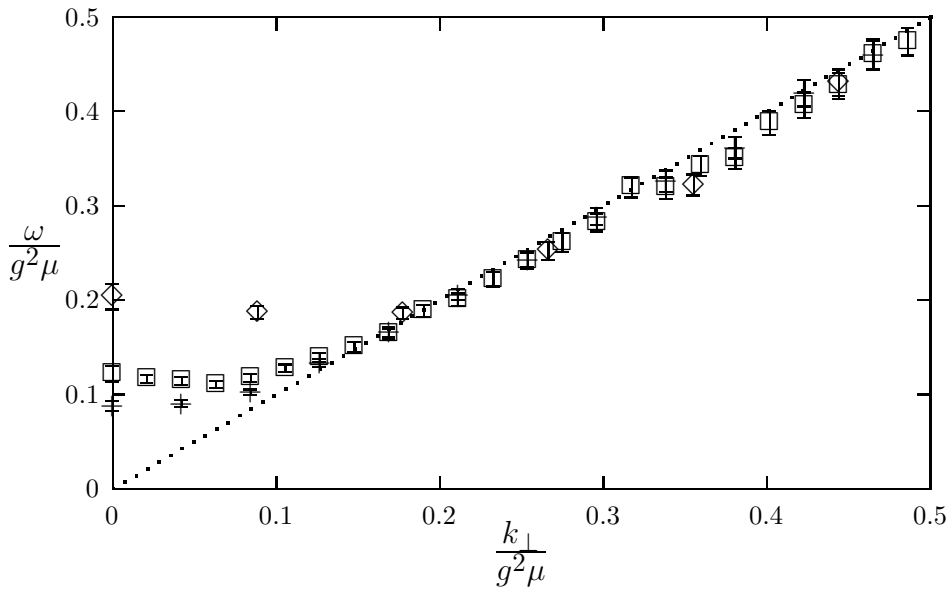


Figure 3: Gluon dispersion relation  $\omega(k_{\perp})$  obtained from Eq. (4), for the values 70.8 (diamonds), 148.5 (plusses), and 297 (squares), with the values of  $g^2 \mu a$  as in Figure 2.